High Pressure Characterization of the Viscous and Volumetric Behavior of Three Transmission Oils

David E.P. Gonçalves,*,† José M. Liñeira del Rio,‡ María J.P. Comuñas,‡ Josefa Fernández,‡ and Jorge H.O. Seabra¶

†*INEGI, Universidade do Porto, Rua Dr. Roberto Frias s/n, 4200-465 Porto, Portugal*

‡*Laboratorio de Propiedades Termofísicas, Grupo NaFoMat, Departamento de Física Aplicada, Universidade de Santiago de Compostela, E-15782 Santiago de Compostela, Spain*

¶*FEUP, Faculdade de Engenharia da Universidade do Porto, Rua Dr. Roberto Frias s/n, 4200-465 Porto, Portugal*

E-mail: degoncalves@inegi.up.pt

Abstract

Measurements of viscosity and density of three lubricating oils (two synthetic and one mineral) were performed. The density of these lubricants was measured at atmospheric pressure by means of a density measuring cell which works on the proven principle of the oscillating tube. Using the same device, the viscosity of these lubricants was measured at 0.1 MPa by using a rotational viscometer.

The volumetric behaviour of the tested lubricants at high pressure is also reported. Density was measured from 278.15 K to 398.15 K up to 120 MPa with a high pressure vibrating tube densimeter. The isobaric thermal expansivity and the isothermal compressibility were determined with a Tammann-Tait equation.

A falling body viscometer was used to determine the viscosity behaviour at high pressure from 303.15 K to 353.15 K up to 150 MPa. From the experimental data obtained in these measurements, the film pressure-viscosity coefficient of these lubricants was calculated and their ability to generate a lubricant film in rolling concentrated contacts was discussed.

Introduction

The main function of a lubricant is to generate a sufficiently thick film, capable of maintaining the separation between moving parts, cooling the contact and minimizing the friction and wear[1,2]. To fulfil that requirement the most important property of a lubricant is its viscosity. Especially in what concerns the elastohydrodynamic (EHL) regime of lubrication, the viscosity variation with temperature and pressure will define the film formation and consequently, the friction and wear of a EHL contact. Thus, the lubricant efficiency for a given application (gears and rolling bearings among others) is function of the load, speed, geometry and mechanical properties of the surfaces which by turn will define the temperature, pressure and shear-rate that the lubricant is subjected to and thus, its viscosity. While the contact operating conditions and the viscosity at atmospheric pressure are generally easy to obtain, the pressure-viscosity coefficient is often unknown, even for the companies which formulate the lubricating oils.

The viscosity variation with pressure can be quantified by the pressure-viscosity coefficient α and the variation with temperature with the temperature-viscosity coefficient β (or in a less scientific approach by the Viscosity Index VI). Both coefficients can be derived from experimental data obtained from atmospheric and high pressure viscometers. Besides viscosity, the density and compressibility are also very important properties for the performance of hydraulic fluids and lubricants in several machines. The efficiency of most pumps can strongly vary with the density and compressibility of the hydraulic fluid[3,4].

The aim of this research work is to analyse the pressure and temperature effects on the

density and viscosity of fully-formulated lubricants and, later on, correlate these properties with their tribological performance. In this manuscript only the measured high pressure properties (viscosity, density and their variations with pressure and temperature) will be reported. To evaluate the suitability of a lubricant in the EHL regime, both properties should be determined in order to be able to predict the film thickness using common expressions derived from numerical simulations[5–11].

The dependence of both viscosity and density with temperature and pressure of three lubricants was experimentally measured and numerically modelled by mathematical equations. The behaviour of each lubricant was then characterized by a set of parameters of those equations, computed from a correlation with the experimental data which was obtained using dedicated test rigs at atmospheric pressure and high-pressure. The physical characterization of these lubricants will be the support of the following part of this work where the relationship between their pressure-viscosity coefficient and their tribological behaviour will be investigated.

Materials and Methods

Tested Lubricants

Three fluids were tested in this work: 75W90 (synthetic nature, API group IV), 80W90 (mineral nature, API group II) and PAO48 (synthetic nature, API group IV). The three of them are commercially available lubricants but their manufactures will not be stated. The lubricating oils 75W90 and 80W90 are fully formulated gear oils which means they contain typical extreme-pressure and anti-wear additives (exact package unknown but they both meet the requirements of API GL-4 and/or GL-5). PAO48 is a non-additized poly-alpha-olefin (PAO) base oil, while 75W90 is a blend of PAO oil and a small amount of Ester.

These lubricants were chosen for this test for the following reasons:

- 75W90 (VI 155) and 80W90 (VI 119) show very similar viscosities, despite their dif-

ferent base oil nature. Furthermore, they are both suitable as transmission gear oils and have similar additive package;

- 75W90 and PAO48 (VI 138) are of the same nature and high VI, but show very different viscosities. Besides, 75W90 has additives while PAO48 does not.

Experimental Techniques

The viscosity, viscosity index and density of the oils at atmospheric pressure were measured with a rotational Anton Paar Stabinger SVM3000. A detailed description of this device was previously reported[12]. Experimental test were performed at 0.1 MPa between 278.15 K and 373.15 K with an experimental uncertainty of 0.0005 g/cm^{-3} for density and a relative expanded uncertainty ($k = 2$) of 1 % for viscosity.

Densities from 278.15 K to 398.15 K up to 120 MPa were determined by using an Anton Paar DMA HPM densimeter. The expanded density uncertainties (at the 95% confidence level, $k = 2$)[13], are 0.7×10^{-3} g/cm^3 at temperatures below T = 373.15 K and pressures up to 120 MPa; 5×10^{-3} g/cm^3 at T = (373.15 and 398.15) K and p = 0.1 MPa and 3×10^{-3} g/cm^3 for T > 373.15 K and p > 0.1 MPa. The setup of the high pressure densimeter is shown in Figure 1.

Density values obtained directly from mechanical oscillator densimeters do not often include the effect that the viscosity sample has on the measurement. In such cases, it is necessary to apply a correction factor to the experimental data, which for the DMA HPM model is given by equation 1[13]:

$$\frac{\rho_{hpm} - \rho}{\rho_{hpm}} = [0.4482 \cdot \sqrt{\eta} - 0.1627] \cdot 10^{-4} \quad (1)$$

where ρ_{hpm} is the density value obtained directly from the densimeter, ρ is the corrected density value, and η is the dynamic viscosity of the liquid in mPa·s. Equation 1 is valid for viscosities lower than 289 mPa·s. For higher viscosities the correction factor is constant, being

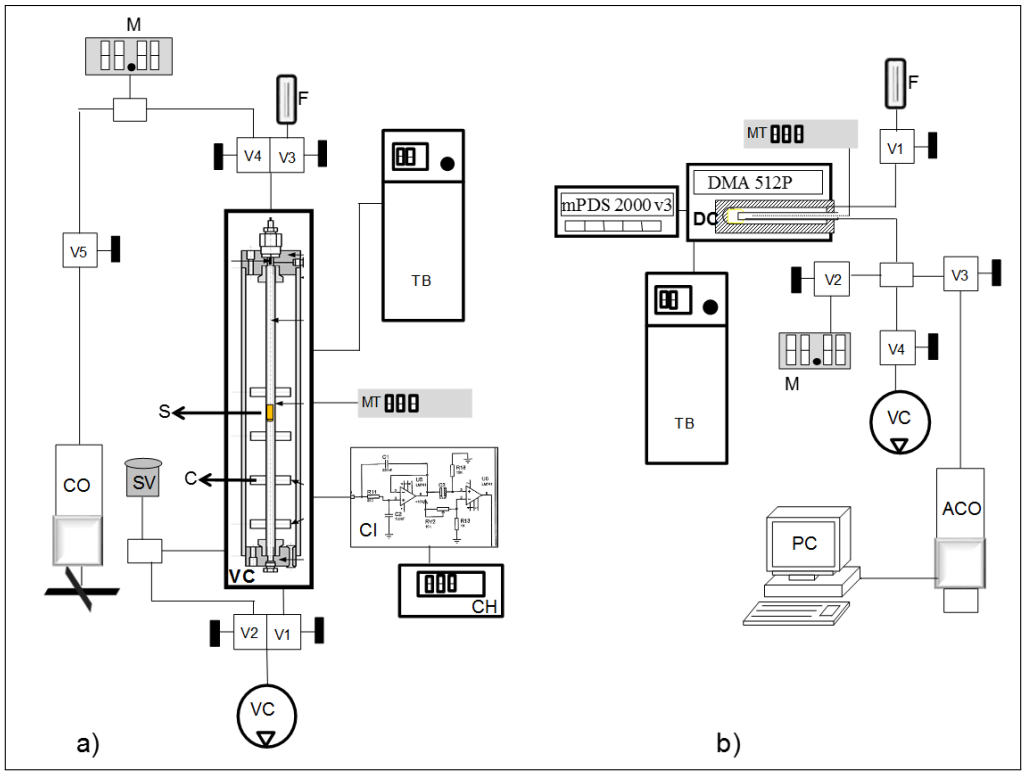

Figure 1: Scheme of the apparatus used for a) viscosity and b) density measurements at high pressure: M= manometer; F= funnel; C= coils; S= Sinker; SV= Safety valve; CO= Compressor; VC= Viscometer Cell; VP= Vacuum Pump; TB= Thermostatic Bath; MT = Agilent Multimeter (PT100 Thermometer); ACO = Automated compressor; PC= Computer; CR= Chronometer; CI= Electronic Circuit.

its value 7.5×10^{-4}. The viscosity values needed in Equation 1 to obtain density correction have been obtained from the correlation shown by Equation 8 reported in this work (using the parameters shown in Table 4), which is based on a modified VFT equation. Given that the experimental temperature and pressure ranges for density (298.15 - 398.15 K) and for viscosity (303.15 - 353.15 K) are not the same, viscosity extrapolation has been considered in order to obtain corrected density values.

Viscosities at high pressure were experimentally determined using a falling body viscometer, VisLPT1, which can operate at pressures up to 150 MPa. More description about this equipment can be seen in previous articles[14–18]. The relative uncertainty of the device from viscosities between 15 mPa.s and 1500 mPa.s is estimated to be 3.5 % with a coverage factor k = 2[14]. The setup of the high pressure viscometer is shown in Figure 1.

Experimental values for squalane determined with this calibration were compared by Dakkach *et al.*[14] with two different correlations proposed by Mylona et al.[19] finding AADs% of 1.41 % and 0.69 %. These deviations confirm the reliability of the equipment.

Experimental results

Atmospheric pressure

Table S1 of the Supporting Information reports the densities and viscosities obtained with the Stabinger apparatus. As shown Figure 2, the mineral oil 80W90 is the one showing the highest density at any temperature. Comparing the synthetic oils, 75W90 shows higher density than PAO48.

The experimental densities at p = 0.1 MPa of each lubricant were fitted to the following equation:

$$\rho_0(T) = A_0 + A_1 \cdot T + A_2 \cdot T^2 \tag{2}$$

In Table 1 the obtained average absolute deviations are gathered together with the parameters involved in Equation 2. For the three oils the AADs% are lower than the apparatus uncertainty. The fact that A_2 shows a very small value indicates that the density's dependence on temperature is almost linear at 0.1 MPa.

Figure 3 shows the measured viscosities for the three oils at 0.1 MPa. The 75W90 and 80W90 oils show very close viscosities at any temperature. At low temperatures the mineral oil has higher viscosity and the opposite is observed at high temperatures due to the

Table 1: Correlation parameters for the density approximation shown in Equation 2.

	75W90	80W90	PAO48
A_0 [g/cm^3]	1.075	1.098	1.019
A_1 $\times 10^{-4}$ [g/cm^3/K]	-7.669	-8.253	-6.798
A_2 $\times 10^{-7}$ [g/cm^3/K^2]	2.045	3.012	1.010
AAD%	0.009	0.046	0.013

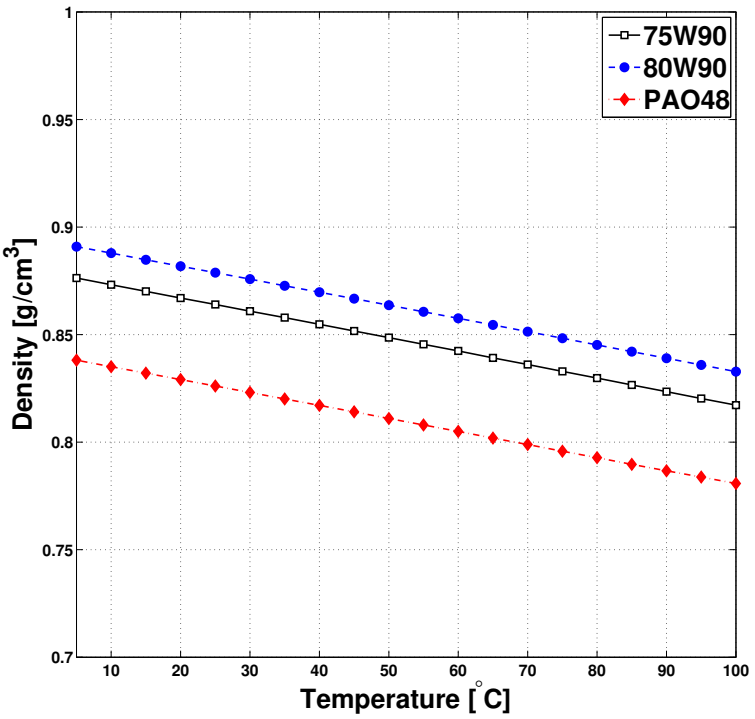

Figure 2: Measured density values of the tested oils as function of the temperature, at atmospheric pressure.

different Viscosity Index of the oils. The PAO48 is the one showing the smallest viscosity for all the temperature range. The viscosity variation with temperature shows an exponential behaviour for all tested lubricants, as expected.

A Vogel-Fulcher-Tammann equation was used to correlate the dynamic viscosities of each oil at atmospheric pressure, as shown in Equation 3.

$$\eta(T) = A \cdot \exp\left(\frac{B}{T - C}\right) \tag{3}$$

Table 2 reports the values of the parameters involved in Equation 3 together with the calculated average absolute deviations, which are lower than the uncertainty of the apparatus for the three oils.

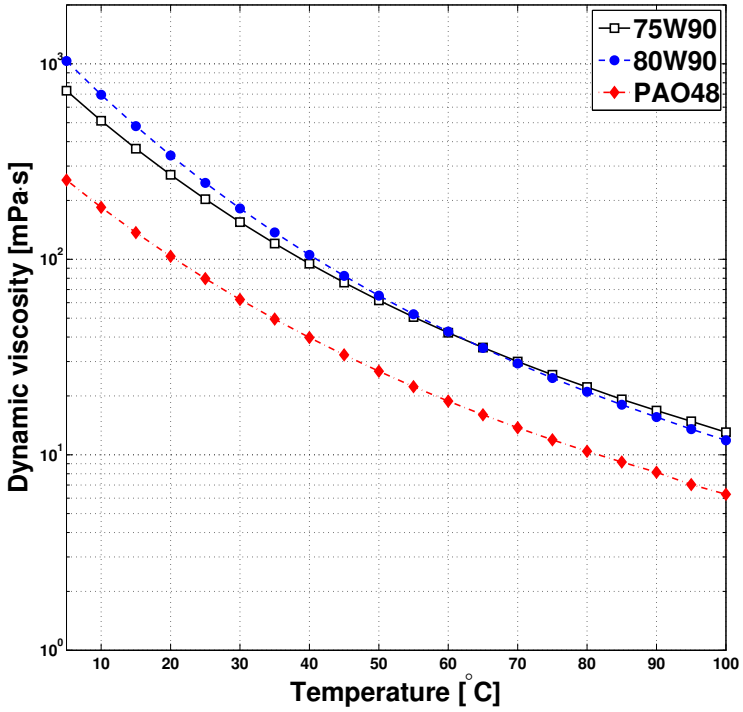

Figure 3: Measured dynamic viscosity of the tested oils as function of temperature, at atmospheric pressure.

Table 2: Correlation parameters for the viscosity approximation shown in Equation 3.

	75W90	80W90	PAO48
A [mPa.s^{-1}]	0.0489	0.0256	0.0327
B [K]	1253.0	1355.9	1203.9
C [K]	147.76	150.29	143.78
AAD%	0.80	1.25	0.59

High-pressure measurements

Density

Figure 4 shows the measured density as a function of pressure and temperature for the tested lubricants. The density data measured at all temperatures and pressures for the three tested lubricants are provided in Table S2 of the Supporting Information. As expected, the density of the three lubricants increases with increasing pressure and decreasing temperature.

Comparing the three tested lubricants, it is clear that the mineral oil 80W90 shows

higher density than the synthetic oils at any temperature or pressure. Comparing 75W90 and PAO48, the former always shows higher density over all the pressure and temperature range.

In order to correlate the density values of the three lubricants as a function of temperature and pressure, a Tait-like Equation was used, as shown in Equation 4[20–24].

$$\rho(p,T) = \frac{\rho_0(T)}{1 - C_0 \cdot \ln\left(\frac{B(T)+p}{B(T)+0.1\ MPa}\right)} \tag{4}$$

with ρ_0(T) obtained from Equation 2 and B(T) being given by Equation 5:

$$B(T) = B_0 + B_1 \cdot T + B_2 \cdot T^2 \tag{5}$$

The values of the parameters A_0, A_1 and A_2 of Equation 2 are obtained from the densities measured at 0.1 MPa with the HPM densimeter. In Table 3 the parameters involved in Equations 4 and 5 are reported.

The curve fitting using Equation 4 is also shown in Figure 4. The deviations of this correlation for each temperature and pressure are shown in Figure S1 of the Supporting Information. Once again the AADs% are very low and the highest deviations (Dmax %) occur only for the measurements performed at the highest temperature (398 K).

Table 3: Correlation parameters and deviations for the density correlation (Equation 4).

	75W90	80W90	PAO48
C_0	0.0835	0.0917	0.0842
B_0 [MPa]	504.15	692.80	456.81
B_1 [MPa/K]	-1.8162	-2.7790	-1.5866
B_2 $\times 10^{-3}$[MPa/K^2]	1.8664	3.2461	1.5705
AAD [%]	0.015	0.057	0.023
Bias [%]	0.002	0.003	0.006
Dmax [%]	0.132	0.193	0.114

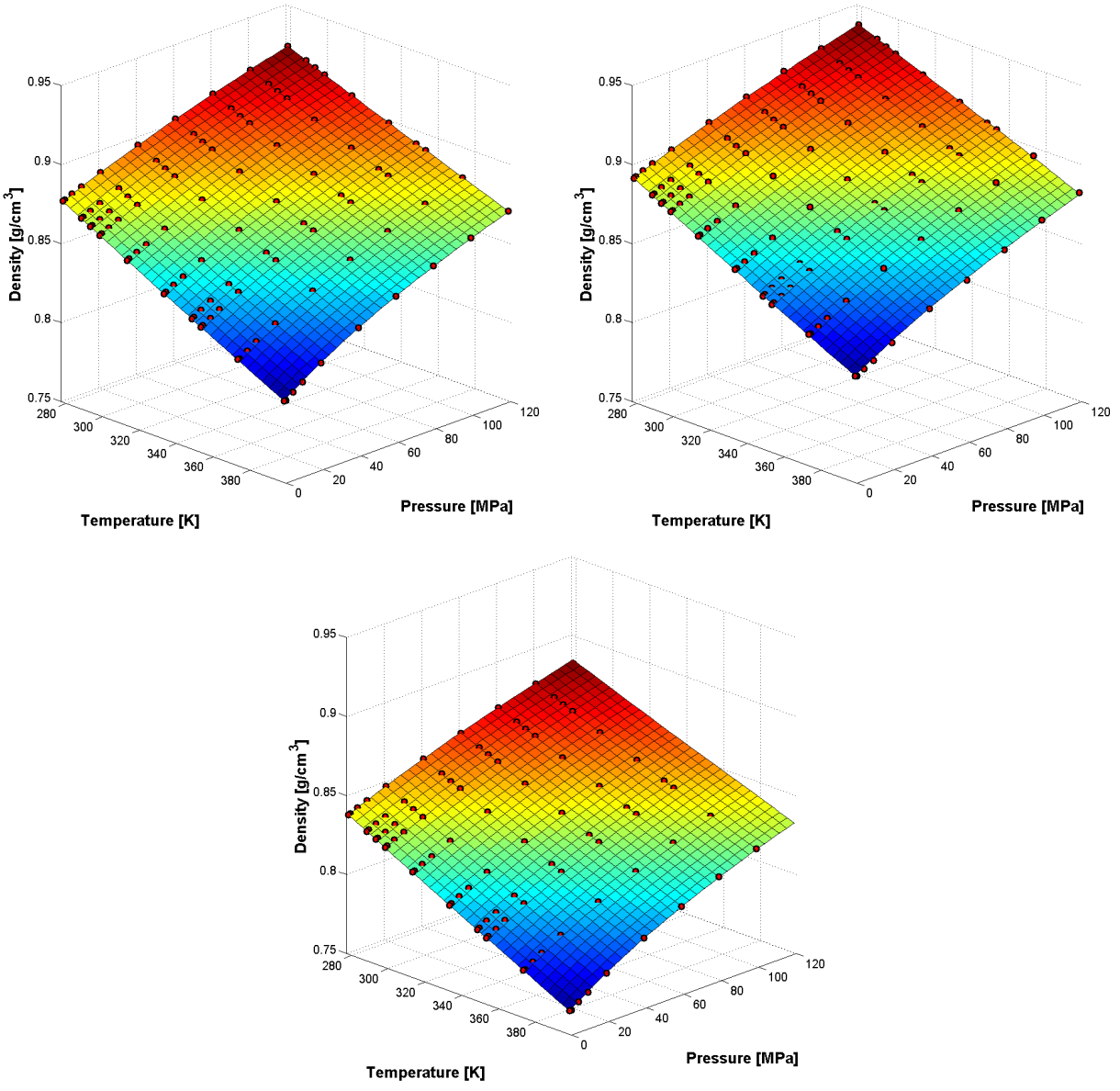

Figure 4: Density of 75W90 as function of temperature and pressure. The red dots represent the measurements and the coloured surface is the correlation of the experimental data using Equation 4.

From the data fitting using Equation 4 it is now possible to calculate the isobaric thermal expansion coefficient α_p through Equation 6, which shows the temperature effect on density at constant pressure.

$$\begin{aligned}\alpha_p = & -\frac{1}{\rho(p,T)}\left(\frac{\partial\rho(p,T)}{\partial T}\right)_p = \\ = & -\frac{d\rho_0(T)}{dT}\frac{1}{\rho_0(T)} - C_0 \cdot \frac{dB(T)}{dT} \cdot \left(\frac{0.1-p}{(B+0.1\ MPa)\cdot(B+p)}\right) \\ & \cdot \left[1 - C_0 \cdot \ln\left(\frac{B(T)+p}{B(T)+0.1\ MPa}\right)\right]^{-1}\end{aligned} \tag{6}$$

Again, from the data fitting using Equation 4, it is also possible to calculate the isothermal compressibility coefficient κ_T through Equation 7, which shows the pressure effect on density at constant temperature:

$$\begin{aligned}\kappa_T = & \frac{1}{\rho(p,T)}\left(\frac{\partial\rho(p,T)}{\partial p}\right)_T = \\ = & \frac{C_0}{(B(T)+p)\cdot\left(1 - C_0 \cdot \ln\left(\frac{B(T)+p}{B(T)+0.1\ MPa}\right)\right)}\end{aligned} \tag{7}$$

The isobaric thermal expansion coefficient α_p and the isothermal compressibility coefficient κ_T are shown in Figure 5 for the whole temperature and pressure range. Both the coefficients decrease with the pressure increase meaning that the higher is the pressure, the less expandable and consequently the less compressible, the fluid is. As for the temperature, the isothermal compressibility coefficient κ_T increases with the temperature increase at constant pressure and it is higher for both the synthetic oils 75W90 and PAO48 by comparison with 80W90.

Figure 5 shows that for the three oils and all the isotherms, the value of $\alpha_p(p)$ decreases with pressure. In addition, it was found that there are several crossing points among the isotherms. This behaviour is quite general and it was the object of controversy [25–27]. Several

75W90

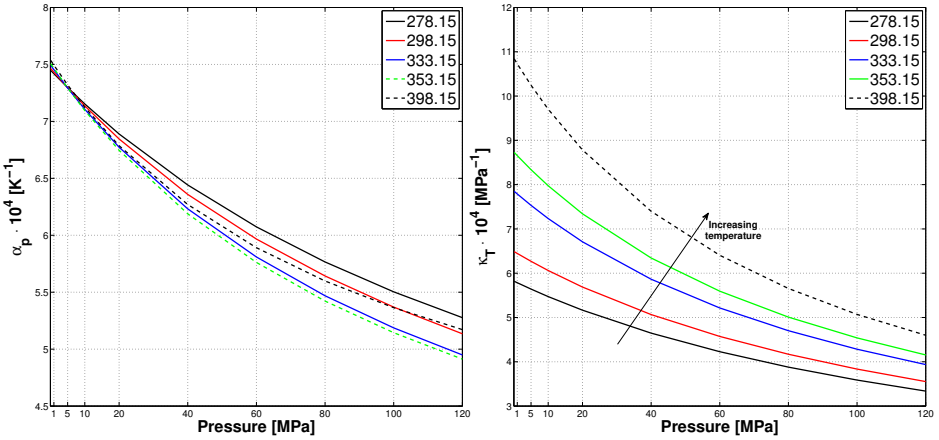

80W90

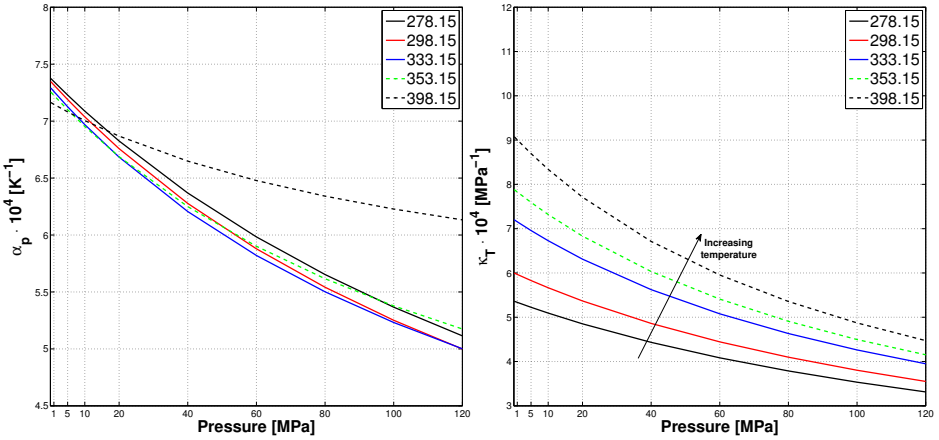

PAO48

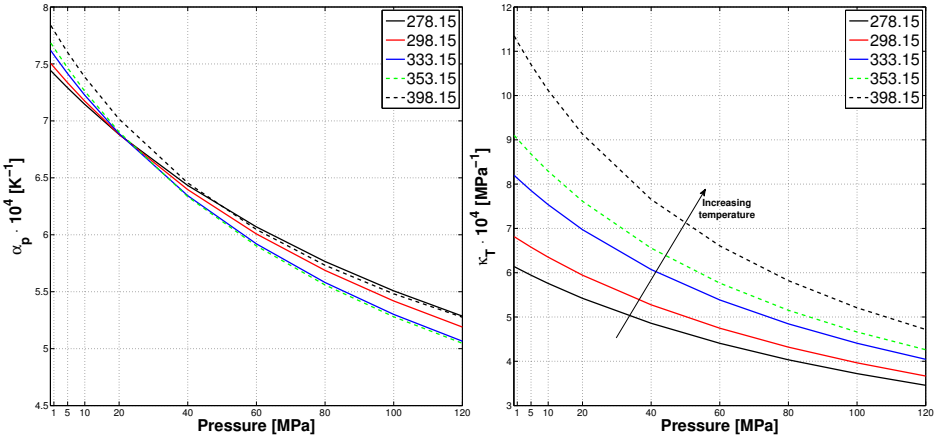

Figure 5: Left Figure: Isobaric thermal expansion coefficient α_p; Right Figure: Isothermal compressibility coefficient κ_T.

authors found that all the studied isotherms of $\alpha_p(p)$ cross in a unique point for many different liquids[13,28–32]. In fact, Deiters and Randzio indicated that an equation of state is valid for a liquid if it can describe a single crossing point for the $\alpha_p(p)$ isotherms[28–30]. On the other hand, Taravillo et al.[33] and Baonza et al.[34] among others[25–27], experimentally found that for some liquids, the $\alpha_p(p)$ isotherms do not show a unique crossing point, at broad temperature ranges. More recently, equations of state derived in the density scaling regime for molecular dynamics as well as Tait-like equations, describe the volumetric data of several liquids in an extremely wide density range, for which several crossing points were found[25–27]. In the present work, using a Tait-like equation (see Equation 4) and experimental data at broad temperature and pressure, it was also found that the volumetric behaviour of these three oils is quite complex, showing several crossing points among the $\alpha_p(p)$ isotherms.

Viscosity

The viscosity of the three oils was experimentally determined by using the falling body viscometer (VISLPT1) at pressures up to 150 MPa and at 303.15, 313.15, 323.15, 333.15, 343.15 and 353.15 K. The density values required to obtain viscosities from the falling times[14] were determined using Equations 2, 4 and 5 and the parameters reported in Tables 1 and 3. At pressures higher than 120 MPa it was necessary to extrapolate density, but this fact does note affect the viscosities at high pressure[15,16].

The dynamic viscosity dependence on pressure and temperature is shown in Figure 6, for the studied lubricants. The viscosity data measured at all temperatures and pressures for the three tested lubricants are available in Table S3 of the Supporting Information.

From the experimental results and as expected, the viscosity of the three lubricants increases with increasing pressure and decreasing temperature. The order of magnitude of the viscosity values at high pressure and low temperature is much higher than those at atmospheric pressure and temperature.

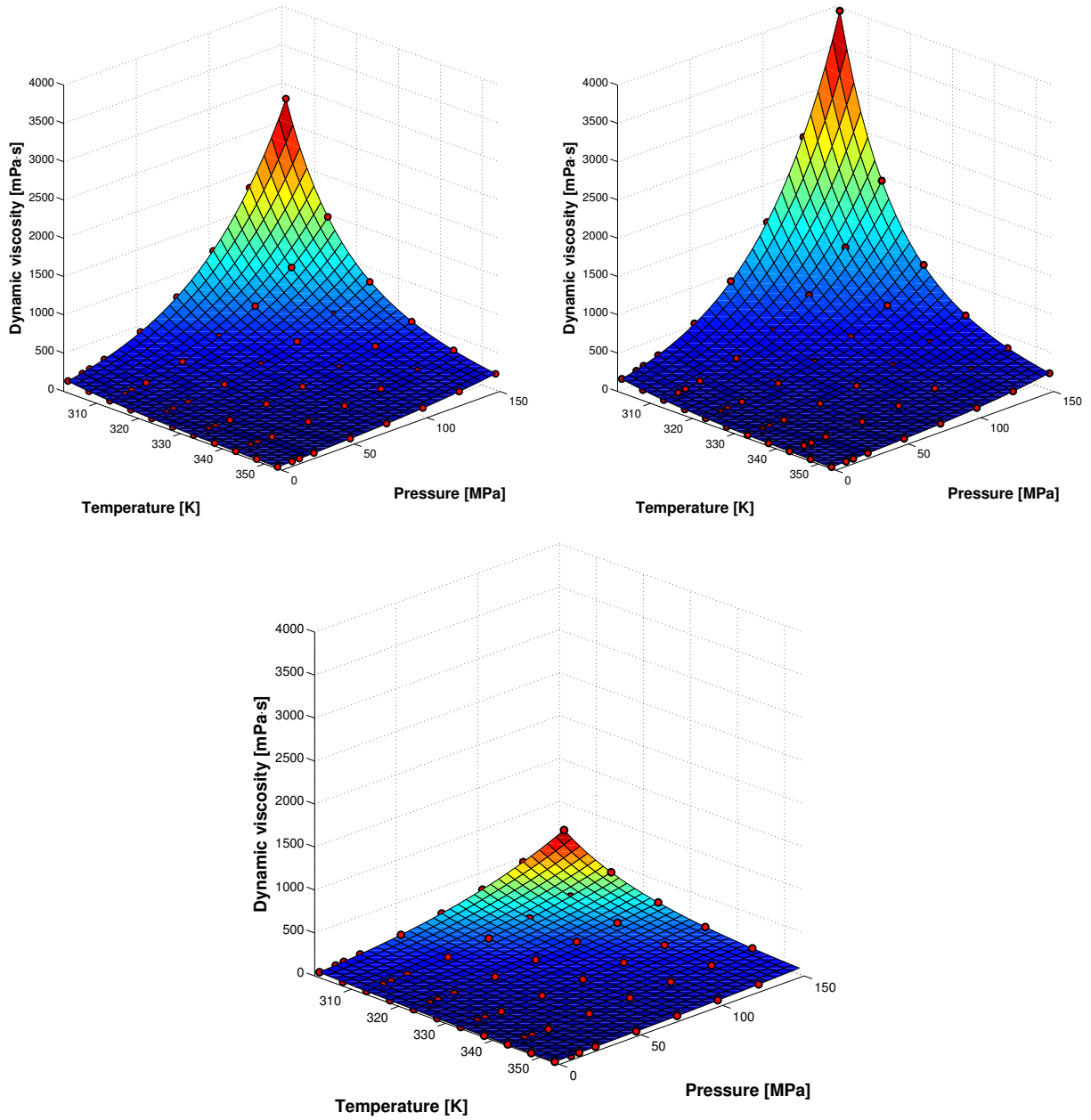

Figure 6: Dynamic viscosity of 75W90 (upper left), 80W90 (upper right) and PAO48 (lower central) as function of temperature and pressure. The red dots represent the measurements and the coloured surface represents the correlation of the experimental data using Equation 8.

The viscosity dependence on temperature at constant pressure and vice-versa is at least exponential. The following modified VFT equation proposed by Comuñas et al[35], which was previously used for several fluids[18,36,37], was employed in this work to correlate the viscosity of the three lubricants against temperature and pressure:

$$\eta(p,T) = A \cdot \exp\left(\frac{B}{T-C}\right) \cdot \left(\frac{p+E(T)}{p_{ref}+E(T)}\right)^{D} \tag{8}$$

The parameters A, B and C are those reported in Table 2, while E(T) has the following form:

$$E(T) = E_0 + E_1 \cdot T + E_2 \cdot T^2 \tag{9}$$

Table 4 report the parameters E0, E1, E2 and D which were obtained from the viscosity values at high-pressures The AADs% are below the expected uncertainty of the device. The curve fitting using Equation 8 is also shown in Figure 6 The deviations of this correlation for each temperature and pressure are shown in Figure S2 of the Supporting Information.

From derivation of Equation 8, it is possible to obtain two coefficients that give information on the effect that temperature and pressure have on viscosity: the local pressure-viscosity $\alpha(p,T)$ (Equation 10) and local temperature-viscosity coefficients $\beta(p,T)$ (Equation 11).

Table 4: Correlation parameters for the viscosity correlation shown in Equation 8.

	75W90	80W90	PAO48
D	9.6896	11.993	6.3890
E_0 [MPa]	-1028.9	-342.38	-372.11
E_1 [MPa/K]	6.6114	2.2891	2.7020
E_2 $\times 10^{-3}$ [MPa/K^2]	-5.9290	1.7497	-1.2871
AAD [%]	1.49	1.34	1.17
Bias [%]	0.28	0.66	-0.35
Dmax [%]	5.99	5.09	4.85

$$\alpha(p,T) = \frac{1}{\eta(p,T)} \left(\frac{\partial\, \eta(p,T)}{\partial p} \right)_T = \frac{D}{E(T)+p} \tag{10}$$

$$\begin{aligned} \beta(p,T) &= -\frac{1}{\eta(p,T)} \left(\frac{\partial\, \eta(p,T)}{\partial T} \right)_p = \\ &= \frac{B}{(T-C)^2} + D\frac{E'(T)\cdot(p-p_{ref})}{(0.1+E(T))\cdot(p+E(T))} \end{aligned} \tag{11}$$

These calculated parameters are represented in Figure 7 and 8 for the tested lubricants at the temperatures of 303.15 K and 353.15 K.

The local pressure-viscosity coefficient decreases when the temperature and the pressure increase for all the tested lubricants, as shown Figure 7. The mineral oil 80W90 shows the highest local pressure-viscosity coefficient at all temperatures as expected from the literature[38–41]. Regarding the synthetic oils, the 75W90 is the one which shows higher local pressure-viscosity coefficient which was also expected since it also shows higher viscosity than PAO48.

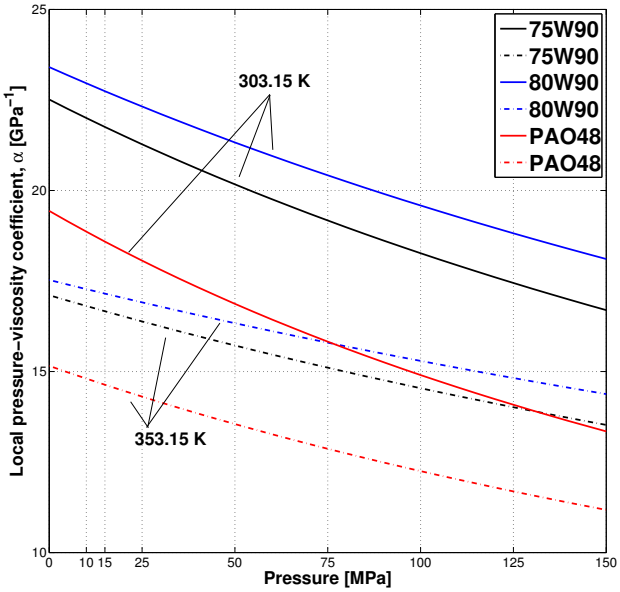

Figure 7: Local pressure-viscosity coefficient α.

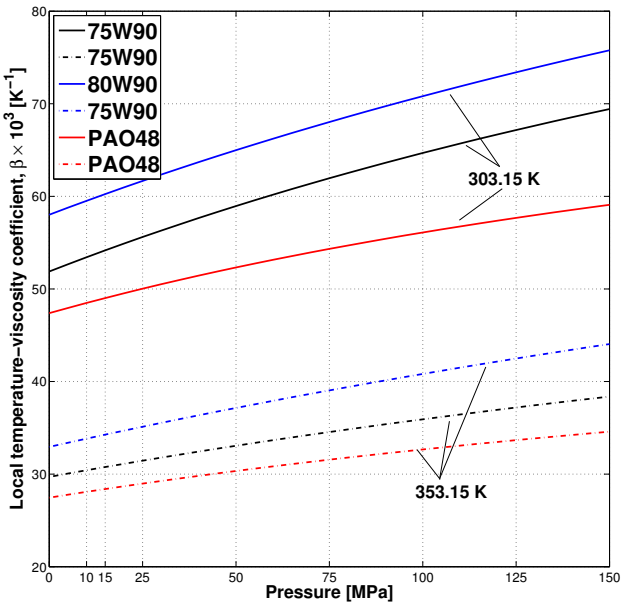

Figure 8: Local temperature-viscosity coefficient β.

On the other hand, Figure 8 shows that the local temperature-viscosity coefficient reaches higher values when the temperature decreases and when the pressure increases. Once again, the mineral oil shows the highest temperature-viscosity coefficient (as expected from a lower VI), followed by the synthetic 75W90 and then the PAO48.

Discussion

Elastohydrodynamic Regime of Lubrication

Under full-film elastohydrodynamic lubrication, if surface material's elastic properties, geometry, roughness and the entrainment speed and load are fixed, two factors affect the central film thickness: the pressure-viscosity coefficient α and the absolute viscosity η_0, as shown in Equation 12:

$$h_{0c} \propto \eta^a \cdot \alpha^b \tag{12}$$

The values of the exponents a and b can change as a function of the contact type being

analysed (elliptical or linear) or even the author or standard considered[5–11]. This α represents the general film forming[42] pressure-viscosity coefficient used to predict the film thickness at any operating temperature, independently of the pressure involved. Other authors use the reciprocal asymptotic isoviscous pressure-viscosity coefficient instead[38,39]. Note that this α parameter is different from the local pressure-viscosity coefficient obtained from Equation 10.

According to Bair et al.[38,39,42,43] the following Equation 13 can be used to estimate the "general film forming pressure-viscosity coefficient" (α_{film}):

$$\alpha = \alpha_{film} = \frac{1 - exp(-3)}{p_{iv}(3/\alpha^*)} \tag{13}$$

where p_{iv} is the isoviscous pressure, given by Equation 14:

$$p_{iv} = \int_0^p \frac{\eta(p' = 0)dp'}{\eta(p')} \tag{14}$$

and α^* is the reciprocal asymptotic isoviscous pressure coefficient[5], calculated with Equation 15.

$$\alpha^* = \frac{1}{p_{iv}(\infty)} = \left[\int_0^{'\infty} \frac{\eta(p = 0)dp}{\eta(p)}\right]^{-1} \tag{15}$$

The comparison between the reciprocal asymptotic isoviscous pressure coefficient α^* and the universal pressure-viscosity coefficient α_{film} is shown in Figure 9 for the three lubricants tested, as function of the temperature. At the Supporting Information, Table S4 reports the values of the α_{film}. It is possible to observe that α_{film} is always higher than α^*. This fact agrees with previous works involving different definitions for the viscosity–pressure coefficient[14,39–41,43]. According to Figure 9, the value of α_{film} and α^* at any temperature, follows the following order:

$$\alpha_{\ 80W90} > \alpha_{\ 75W90} > \alpha_{\ PAO48}$$

Assuming that a relationship between the viscosity and the pressure-viscosity coefficient can be accurately established, it is possible to use Equation 16 proposed by Gold *et al.*[44], to estimate the pressure-viscosity coefficient knowing the kinematic viscosity (ν) and the nature of each oil formulation.

$$\alpha_{film} = s \cdot \nu^t \cdot 10^{-8} \tag{16}$$

Minimizing the different between the experimental results shown in Figure 9 and the results obtained with Equation 16, it is possible to optimize the (s,t) parameters for each tested oil. Table 5 shows the (s,t) values found and the AAD% from the experimental results. It is interesting to notice that the synthetic oils shows similar (s,t) parameters between them.

Figure 10 shows the product of the viscosity and pressure-viscosity coefficient with the exponents proposed by Hamrock and Downson for a Hard EHL elliptical contact[5]. This product $\eta^{0.67} \cdot \alpha^{0.53}$ represents the ability to form a lubricant film for fixed geometry, operating

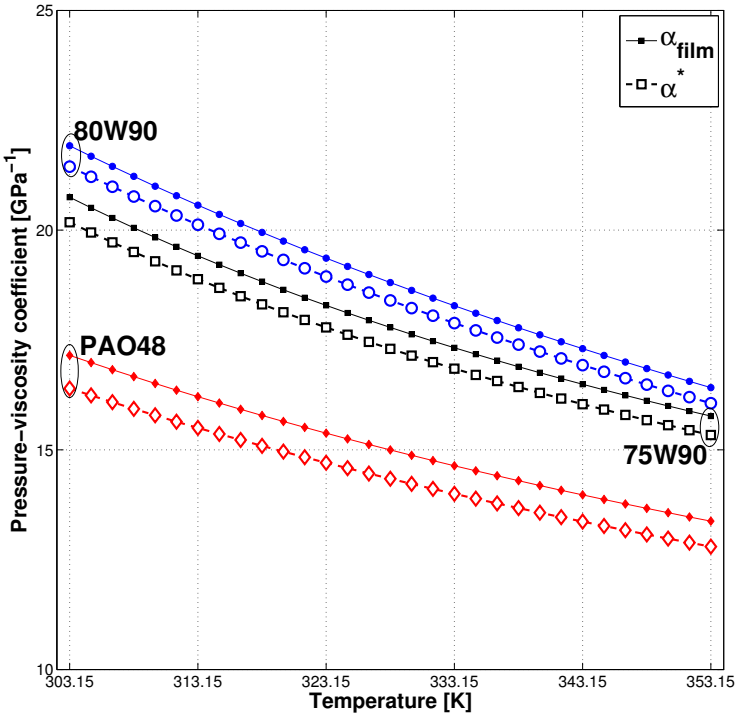

Figure 9: Comparison between α_{film} and α^* as function of temperature for the three tested lubricants.

Table 5: Optimized (s,t) parameters, according to Equation 16[44].

	75W90	80W90	PAO48
s	9.840	10.637	9.352
t	0.144	0.137	0.141
AAD%	0.875	2.749	1.738

conditions and temperature: the higher it is, the higher should be the film thickness.

It is possible to observe that the 80W90 oil shows a combination of higher viscosity and higher pressure-viscosity coefficient at low temperatures and therefore should also show higher film thickness. However, since both these properties decrease quicker with temperature for 80W90 than for 75W90, at higher temperatures (above 333.15 K) their film thickness should be very similar or even higher for the 75W90 oil. The PAO48 is the one which always shows smaller $\eta^{0.67} \cdot \alpha^{0.53}$ at any temperature, due to its much smaller viscosity.

Given that 75W90 and 80W90 are both suitable as transmission gear oils and 80W90 is actually a cheaper substitute for 75W90, it is interesting to notice that between 333.15-

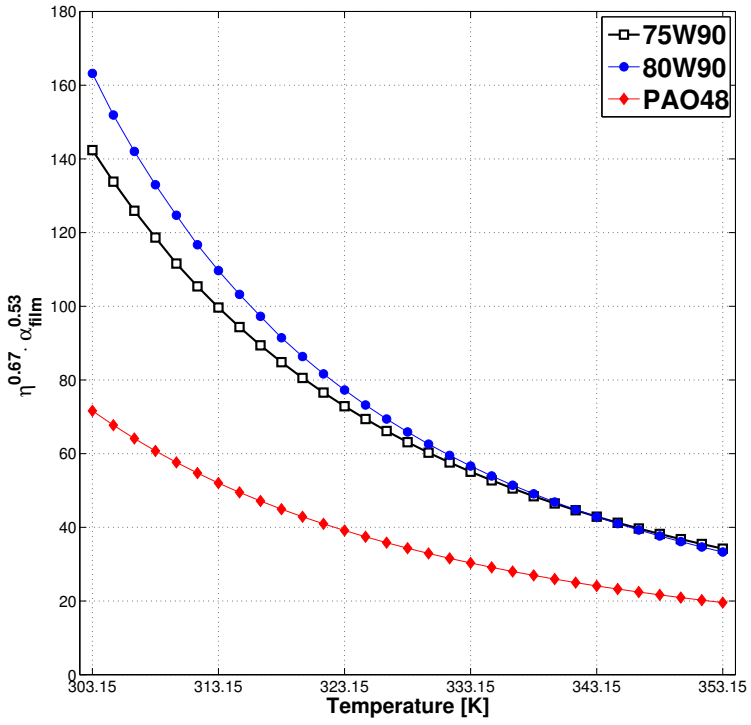

Figure 10: $\eta^{0.67} \cdot \alpha^{0.53}$ parameter as function of the temperature for the tested lubricants.

353.15 K (the typical operating temperature of a rear wheel-drive automotive gearbox), their performances should be very similar. These oils show similar ($\eta^{0.67} \cdot \alpha^{0.53}$) which indicates that they should produce very similar film thickness at this temperature and therefore also similar performance in terms of wear and friction. At lower operating temperatures, due to increased viscosity and pressure-viscosity coefficient, 80W90 should show higher viscous friction producing higher churning losses and power loss.

However, in what concerns friction, other authors found a relationship between the α_{film} of several oils and the friction coefficient measured in simple ball-on-disc tests using those oils[45,46]. Brandão et al. has even proposed a modification of the typical Hersey-Stribeck parameter in order to include the effect of the pressure-viscosity coefficient and thus, better represent the friction coefficient as function of the operating conditions and the lubricant properties[47]. Therefore, even if these two oils produce the same film thickness above 333.15 K, the one showing the highest α_{film} should also show higher values of friction coefficient in full film elastohydrodynamic lubrication. Outside this region (mixed or even boundary film lubrication), the viscosity should be less relevant and the additive package starts to take a more important role.

The relation between the friction and film thickness, associated with the pressure-viscosity coefficient, will be the scope of future works.

Conclusions

The physical properties (density and viscosity) of three different lubricants were measured in dedicated test rigs from atmospheric pressure up to 150 MPa for a wide temperature range. Numerical models were then successfully correlated with the experimental data, describing the volumetric and viscous behaviour with temperature and pressure for each lubricant.

From these correlations, other parameters were derived numerically as the isobaric thermal expansion coefficient α_p, the isothermal compressibility coefficient κ_T, the local pressure-

viscosity coefficient α and temperature-viscosity coefficient β. These properties describe the lubricants' behaviour with temperature and pressure which are important to understand if these fluids are suitable for hydraulic applications and also their tribological behaviour in an EHL contact.

It was found that the mineral oil tested shows higher density and smaller isothermal compressibility coefficient than the synthetic oils tested for the whole temperature and pressure range. The knowledge of the viscosity variation over temperature and pressure allowed for the calculation of the film pressure-viscosity coefficient over a wide temperature range. Once again, the mineral oil showed higher α_{film} at any temperature than the synthetic oils tested.

The film pressure-viscosity coefficient, coupled with the viscosity at each temperature ($\eta^{0.67} \cdot \alpha^{0.53}$), represents the film forming ability of each lubricant. In this case, it was found that the mineral oil 80W90 shows a higher value of this parameter than the synthetic oil 75W90 at temperatures below 343.15 K and equal or even smaller from this temperature onwards.

Acknowledgement

The authors gratefully acknowledge the funding through several projects and grants without whom this work would not have been possible:

- IACOBUS exchange program (2017);
- ENE2014-55489-C2-1-R and ENE2017-86425-C2-2-R co-financed by the Spanish Ministry of Economy and Competitiveness and the European ERDF programme;
- GRC ED431C 2016/001 financed by Xunta de Galicia (Spain);
- AGRUP2015/11 financed by Xunta de Galicia (Spain);
- Principia program JMLR of Xunta de Galicia (Spain);

- NORTE-01-0145-FEDER-000022 - SciTech - Science and Technology for Competitive and Sustainable Industries, cofinanced by Programa Operacional Regional do Norte (NORTE2020), through Fundo Europeu de Desenvolvimento Regional (FEDER);

- LAETA under the project UID/EMS/50022/2013.

Supporting Information Available

The following files are available free of charge.

- Supporting Information: Tables containing the Viscosity and Density data for all the tested lubricants under atmospheric pressure and high-pressure (up to 150 MPa).

References

(1) Reynolds, O. On the Theory of Lubrication and Its Application to Mr. Beauchamp Tower's Experiments, Including an Experimental Determination of the Viscosity of Olive Oil. *Proc. R. Soc. Lond.* **1886**, *177*, 191–203.

(2) Stribeck, R.; Schröter, M. *Die wesentlichen Eigenschaften der Gleit-und Rollenlager: Untersuchung einer Tandem-Verbundmaschine von 1000 PS*; Springer, 1903.

(3) Lawate, S. In *Environmentally Friendly Hydraulic Fluids in Biobased Industrial Fluids and Lubricants*; Sevim Z. Erhan, J. M. P., Ed.; p Chapter 3.

(4) Rudnick, L. R. *Synthetics, mineral oils, and bio-based lubricants: chemistry and technology*; Chemical Industries; Taylor & Francis, 2005.

(5) Hamrock, B. J.; Dowson, D. Isothermal Elastohydrodynamic Lubrication of Point Contacts Part III—Fully Flooded Results. *Journal of Lubrication Technology* **1977**, *99*, 264.

(6) Chittenden, R. J.; Dowson, D.; Dunn, J. F.; Taylor C., M. A theoretical analysis of the isothermal elastohydrodynamic lubrication of concentrated contacts, part I: direction of lubricant entrainment coincident with the major axis of the Hertzian contact ellipse. *Proc. R. Soc. Lond* **1985**, *A397(1813)*, 245–269.

(7) Gohar, R. Oil Film Thickness and Rolling Friction in Elastohydrodynamic Point Contact. *Journal of Lubrication Technology* **1971**, *93*, 371.

(8) Higginson, G. R.; Dowson, D. A Numerical Solution to the Elasto-Hydrodynamic Problem. *Journal Mechanical Engineering Science* **1965**, *7*, 5.

(9) Ranger, A. P.; Ettles, C. M. M.; Cameron, A. The Solution of the Point Contact Elasto-Hydrodynamic Problem. *Proceedings of the Royal Society of London. A. Mathematical and Physical Sciences* **1975**, *346*, 227 LP – 244.

(10) Hooke C., J. The Elastohydrodynamic Lubrication of Heavily Loaded Contacts. *Journal of Mechanical Engineering Science* **1977**, *19*, 149–156.

(11) Evans, H. P.; Snidle, R. W. The isothermal elastotohydrodynamic lubrication of spheres. **1981**, *103*.

(12) Gaciño, F. M.; Regueira, T.; Lugo, L.; Comuñas, M. J.; Fernández, J. Influence of Molecular Structure on Densities and Viscosities of Several Ionic Liquids. *Journal of Chemical & Engineering Data* **2011**, *56*, 4984–4999.

(13) Segovia, J. J.; Fandiño, O.; López, E. R.; Lugo, L.; Carmen Martín, M.; Fernández, J. Automated densimetric system: Measurements and uncertainties for compressed fluids. *Journal of Chemical Thermodynamics* **2009**, *41*, 632–638.

(14) Dakkach, M.; Gaciño, F.; Guimarey, M. J.; Mylona, S. K.; Paredes, X.; Comuñas, M. J.; Fernández, J.; Assael, M. J. Viscosity-pressure dependence for nanostructured ionic liquids. Experimental values for butyltrimethylammonium and 1-butyl-

3-methylpyridinium bis(trifluoromethylsulfonyl)imide. *Journal of Chemical Thermodynamics* **2018**, *121*, 27–38.

(15) Gaciño, F. M.; Paredes, X.; Comuñas, M. J.; Fernández, J. Effect of the pressure on the viscosities of ionic liquids: Experimental values for 1-ethyl-3-methylimidazolium ethylsulfate and two bis(trifluoromethyl- sulfonyl)imide salts. *Journal of Chemical Thermodynamics* **2012**, *54*, 302–309.

(16) Gaciño, F. M.; Paredes, X.; Comuñas, M. J.; Fernández, J. Pressure dependence on the viscosities of 1-butyl-2,3-dimethylimidazolium bis(trifluoromethylsulfonyl)imide and two tris(pentafluoroethyl) trifluorophosphate based ionic liquids: New measurements and modelling. *Journal of Chemical Thermodynamics* **2013**, *62*, 162–169.

(17) Comuñas, M. J.; Paredes, X.; Gaciño, F. M.; Fernández, J.; Bazile, J. P.; Boned, C.; Daridon, J. L.; Galliero, G.; Pauly, J.; Harris, K. R. Viscosity measurements for squalane at high pressures to 350 MPa from T = (293.15 to 363.15) K. *Journal of Chemical Thermodynamics* **2014**, *69*, 201–208.

(18) Gaciño, F. M.; Comuñas, M. J.; Regueira, T.; Segovia, J. J.; Fernández, J. On the viscosity of two 1-butyl-1-methylpyrrolidinium ionic liquids: Effect of the temperature and pressure. *Journal of Chemical Thermodynamics* **2015**, *87*, 43–51.

(19) Wang, S.; Jacquemin, J.; Husson, P.; Hardacre, C.; Costa Gomes, M. F. Liquid-liquid miscibility and volumetric properties of aqueous solutions of ionic liquids as a function of temperature. *Journal of Chemical Thermodynamics* **2009**, *41*, 1206–1214.

(20) Regueira, T.; Lugo, L.; Fernández, J. Ionic liquids as hydraulic fluids: comparison of several properties with those of conventional oils. *Lubrication Science* **2009**, 123–134.

(21) Gaciño, F. M.; Regueira, T.; Comuñas, M. J.; Lugo, L.; Fernández, J. Density and isothermal compressibility for two trialkylimidazolium-based ionic liquids at temperatures

from (278 to 398) K and up to 120 MPa. *Journal of Chemical Thermodynamics* **2015**, *81*, 124–130.

(22) Gaciño, F. M.; Regueira, T.; Bolotov, A. V.; Sharipov, A.; Lugo, L.; Comuñas, M. J.; Fernández, J. Volumetric behaviour of six ionic liquids from T = (278 to 398) K and up to 120 MPa. *Journal of Chemical Thermodynamics* **2016**, *93*, 24–33.

(23) Regueira, T.; Lugo, L.; Fernández, J. Influence of the pressure, temperature, cation and anion on the volumetric properties of ionic liquids: New experimental values for two salts. *Journal of Chemical Thermodynamics* **2013**, *58*, 440–448.

(24) Regueira, T.; Lugo, L.; Fernández, J. High pressure volumetric properties of 1-ethyl-3-methylimidazolium ethylsulfate and 1-(2-methoxyethyl)-1-methylpyrrolidinium bis(trifluoromethylsulfonyl)imide. *Journal of Chemical Thermodynamics* **2012**, *48*, 213–220.

(25) López, E. R.; Fandiño, O.; Cabaleiro, D.; Lugo, L.; Fernández, J. Determination of derived volumetric properties and heat capacities at high pressures using two density scaling based equations of state. Application to dipentaerythritol hexa(3,5,5-trimethylhexanoate). *Physical Chemistry Chemical Physics* **2018**, *20*, 3531–3542.

(26) Chorążewski, M.; Grzybowski, A.; Paluch, M. The complex, non-monotonic thermal response of the volumetric space of simple liquids. *Phys. Chem. Chem. Phys.* **2014**, *16*, 19900–19908.

(27) Chorązewski, M.; Grzybowski, A.; Paluch, M. Isobaric Thermal Expansion of Compressed 1,4-Dichlorobutane and 1-Bromo-4-chlorobutane: Transitiometric Results and a Novel Application of the General Density Scaling-Based Equation of State. *Industrial and Engineering Chemistry Research* **2015**, *54*, 6400–6407.

(28) Randzio, S. L. From Calorimetry to Equations of State. *Chemical Society Reviews* **1995**,

(29) Randzio, S. L.; Deiters, U. K. Thermodynamic Testing of Equations of State of Dense Simple Liquids. *Ber. Bunsenges. Phys. Chem.* **1995**, *99*, 1179–1186.

(30) Deiters, U. K.; Randzio, S. L. The equation of state for molecules with shifted Lennard-Jones pair potentials. *Fluid Phase Equilibria* **1995**, *103*, 199–212.

(31) Valencia, L.; Gonza, D.; Troncoso, J.; Carballo, E. Thermophysical Characterization of Liquids Using Precise Density and Isobaric. **2009**, 904–915.

(32) Cerdeiriñ, C. A.; Tovar, C. A.; González-Salgado, D.; Carballo, E.; Romaní, L. Isobaric thermal expansivity and thermophysical characterization of liquids and liquid mixturesy. *Physical Chemistry Chemical Physics* **2001**, *3*, 5230–5236.

(33) Taravillo, M.; Baonza, G.; C, M. Thermodynamic regularities in compressed liquids : I . The thermal expansion coefficient Javier N u. **2003**, *15*, 2979–2989.

(34) García Baonza, V.; Cáceres, M.; Núñez, J. The spinodal as a reference curve for the high-pressure volumetric behavior of liquids. *Chemical Physics Letters* **1993**, *216*, 579–584.

(35) Comuñas, M. J.; Baylaucq, A.; Boned, C.; Fernández, J. High-pressure measurements of the viscosity and density of two polyethers and two dialkyl carbonates. *International Journal of Thermophysics* **2001**, *22*, 749–768.

(36) Paredes, X.; Pensado, A. S.; Comuñas, M. J.; Fernández, J. Experimental dynamic viscosities of dipentaerythritol ester lubricants at high pressure. *Journal of Chemical and Engineering Data* **2010**, *55*, 3216–3223.

(37) Schmidt, K. A. G.; Pagnutti, D.; Curran, M. D.; Singh, A.; Trusler, J. P. M.; Maitland, G. C.; McBride-Wright, M. Erratum: New Experimental Data and Reference Models for the Viscosity and Density of Squalane (J. Chem. Eng. Data (2015) 60:1

(137-150) (10.1021/je5008789). *Journal of Chemical and Engineering Data* **2016**, *61*, 698.

(38) Bair, S.; Qureshi, F. Accurate measurements of pressure-viscosity behavior in lubricants. *Tribology Transactions* **2002**, *45*, 390–396.

(39) Scott Bair, P. E. *High-pressure rheology for quantitative elastohydrodynamics*; Elsevier, 2007; p 240.

(40) Paredes, X.; Fandiño, O.; Pensado, A. S.; Comuñas, M. J.; Fernández, J. Pressure-viscosity coefficients for polyalkylene glycol oils and other ester or ionic lubricants. *Tribology Letters* **2012**, *45*, 89–100.

(41) Pensado, A. S.; Comuñas, M. J.; Fernández, J. The pressure-viscosity coefficient of several ionic liquids. *Tribology Letters* **2008**, *31*, 107–118.

(42) Björling, M.; Bair, S.; Mu, L.; Zhu, J.; Shi, Y. Elastohydrodynamic Performance of a Bio-Based, Non-Corrosive Ionic Liquid. *Applied Sciences* **2017**, *7*, 996.

(43) Bair, S. Reference liquids for quantitative elastohydrodynamics: Selection and rheological characterization. *Tribology Letters* **2006**, *22*, 197–206.

(44) Gold, P. W.; Schmidt, A.; Dicke, H.; Loos, J.; Assmann, C. Viscosity–pressure–temperature behaviour of mineral and synthetic oils. *Journal of Synthetic Lubrication* **2001**, *18*, 51–79.

(45) Brandão, J. A.; Meheux, M.; Seabra, J. H. O.; Ville, F.; Castro, M. J. D. Traction curves and rheological parameters of fully formulated gear oils. *Proceedings of the Institution of Mechanical Engineers, Part J: Journal of Engineering Tribology (in press)* **2011**, *225*, 577–593.

(46) Brandão, J. A.; Meheux, M.; Ville, F.; Castro, J.; Seabra, J. Experimental traction and Stribeck curves of mineral, PAO and ester based fully formulated gear oils. *In: Pro-*

ceedings of the 3rd International Conference on Integrity, Reliability & Failure, Porto, Portugal, **2009**,

(47) Brandão, J. A.; Meheux, M.; Ville, F.; Seabra, J. H.; Castro, J. Comparative overview of five gear oils in mixed and boundary film lubrication. *Tribology International* **2012**, *47*, 50–61.

For Table of Contents Only

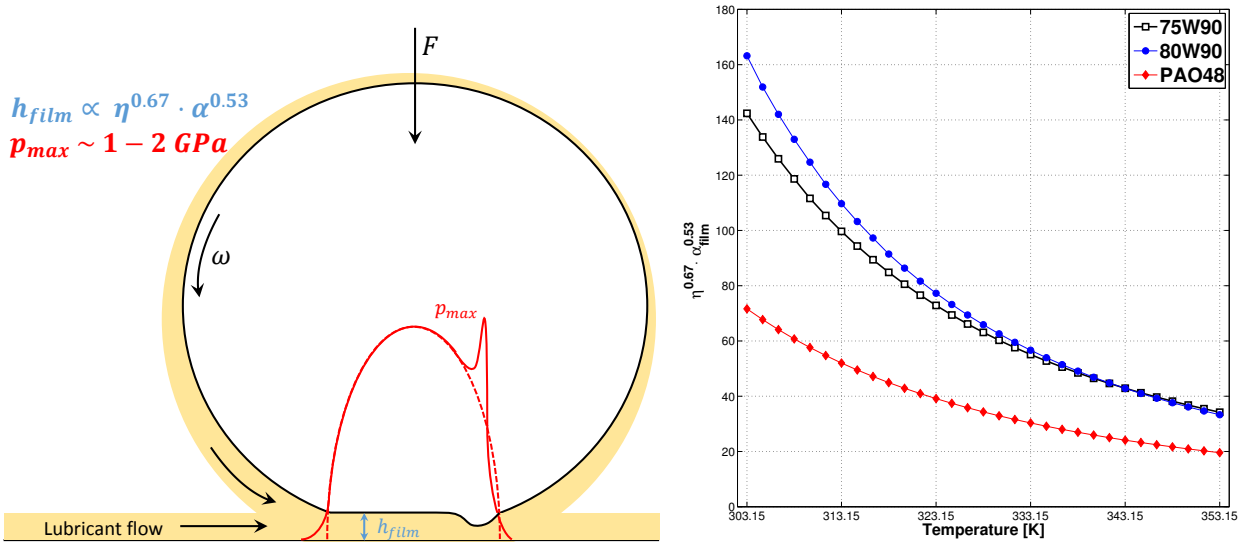

Figure 11: For Table of Contents Only